Color-singlet quark-pair transmutation: Helicity amplitudes and partial-wave analysis

W. Roberts*
Guelph-Waterloo Program for Graduate Work in Physics, Department of Physics, University of Guelph, Guelph, Ontario, Canada N1G 2W1
(Received 16 August 1988)

Quark-pair transmutation via two gluons is the lowest-order, color-singlet process. In this paper the helicity amplitudes for this process are evaluated and a partial-wave analysis performed. The amplitudes for these annihilations are infrared divergent and this divergence is removed by giving the gluons a confinement mass. The results are generally dependent on this mass. Many of the features are similar to those of quark-pair annihilation into two gluons. Somewhat surprisingly, there is a large proportion of a 1^+ partial wave. Threshold effects are understood in terms of threshold effects in pair annihilation into two gluons. However, there is a "competition" effect that depends on the ratio of masses of the initial- and final-quark pairs. For similar masses, singlet production dominates as expected, but for very dissimilar masses, singlet annihilation of the heavier pair competes with triplet production of the lighter pair. Some comments about the possible applications and extensions of this work are made. Obvious applications are to the Okubo-Zweig-Iizuka-rule-suppressed decays of quarkonia. Other applications include development of a quark-pair-creation model that differs from the usual $^3P_0$ and $^3S_1$ models.

I. INTRODUCTION AND MOTIVATION

Quark-pair annihilation and production are two of the most important subprocesses occurring in hadron physics. Formation of hadron jets, as well as the production of heavy quarkonia from two photons, proceed via quark-antiquark production as an intermediate step. In hadron colliders such as proton-antiproton machines, quark-antiquark annihilation is one of the dominant subprocesses leading to formation of the various resonances and jets observed. Quark-pair production also occurs in the Okubo-Zweig-Iizuka[1]- (OZI-) rule-allowed decays of quarkonia, while both annihilation and production occur in the OZI-suppressed decays.

Two phenomenological models have been developed for description of the pair-creation process. In these models, the created pair is in a partial wave that is determined by the mechanism of creation for the pair: $^3S_1$ for pair creation from a single gluon[2] or $^3P_0$ for pair creation out of the QCD vacuum.[3]

Both these models have been applied, with numerous modifications and moderate success, to other hadron processes. However, in both models the choice of partial wave of the created pair is based on somewhat *ad hoc* assumptions about how the pair is created. While both assumptions may have some degree of validity, neither of them gives the complete physical picture of pair creation. Perhaps this is why both models appear to have problems in describing $p\bar{p}$ annihilation, for instance.[4]

Within the framework of QCD, the essentially nonperturbative $^3S_1$ model may be thought of as being based on the first term in a perturbative treatment of pair production. The next logical step should be an investigation of two-gluon pair production. This would allow two objectives to be realized. The first is the obvious extension of the "perturbative" series, and the possible refinements this may allow. This is quite useful since, even though the pair-creation models may themselves be nonperturbative, many features of the perturbative treatment are expected to carry over into the nonperturbative regime. A study of the perturbative description of pair creation will thus lead to a better understanding of the dynamics of the nonperturbative process.

The second objective is the fact that any model based on the two-gluon amplitudes is also valid for the regime of perturbative QCD, and would thus be particularly applicable to discussions of high-energy subprocesses, as well as production and/or annihilation of heavy-quark pairs.

In this paper, the two-gluon process, namely, $q\bar{q}\to gg\to Q\bar{Q}$, is studied with the aid of helicity amplitudes and a partial-wave analysis. The use of helicity amplitudes facilitates the discussion of spin effects, which are significant at all energies. The threshold and high-energy behavior are discussed in detail. The development of a model similar to the ones mentioned above is left for future work.

The two-gluon process, with the appropriate choice of color factors, is the lowest-order color-singlet annihilation and production process. This provides added motivation for its study, as it is then easily and directly applicable to decays of quarkonia, as well as to mixing between quarkonia states. For the sake of simplicity, the color-singlet process alone will be discussed.

Sections III–V of this paper present the detailed treatment of $q\bar{q}\to Q\bar{Q}$. Sections VI and VII present a summary of the main results of the calculation, as well as some comments and conclusions. Possible applications are also discussed in Sec. VII. Three appendixes present some details of the helicity amplitudes and partial-wave analysis.

II. SYMMETRIES AND SELECTION RULES

The helicity of a particle is defined as the component of the spin of that particle along its direction of motion.[5] For spin-$\frac{1}{2}$ fermions, there are two possible helicities, which may be denoted as $\pm$. The four possible two-particle helicity states are $|++\rangle$, $|+-\rangle$, $|-+\rangle$, and $|--\rangle$.

These two-fermion helicity states are not, however, eigenstates of parity or charge conjugation. Such eigenstates are easily constructed and they are[6]

$$\begin{aligned}
|1\rangle &= (|++\rangle + |--\rangle)/\sqrt{2} \quad [(-1)^J] \quad ({}^3P_0, {}^3P_2) ,\\
|2\rangle &= (|++\rangle - |--\rangle)/\sqrt{2} \quad [(-1)^{J+1}] \quad ({}^1S_0, {}^1D_2) ,\\
|3\rangle &= (|+-\rangle + |-+\rangle/\sqrt{2} \quad [(-1)^J] \quad ({}^3P_2, {}^3F_2) ,\\
|4\rangle &= (|+-\rangle - |-+\rangle)/\sqrt{2} \quad [(-1)^{J+1}] \quad ({}^3P_1, {}^3F_3) .
\end{aligned} \tag{1}$$

The quantities in square brackets are the parity eigenvalues of the states, and the $\sqrt{2}$ is a normalization factor. Two of the angular momentum states to which each parity eigenstate contributes are also shown. Note that partial waves such as ${}^1P_1$ and ${}^1F_3$, corresponding to $J^{PC}=1^{+-}$ and 3^{+-}, respectively, are not allowed for the two-gluon, color-singlet process since charge conjugation is even for such a process.

For the process of interest, let the initial pair define the z axis in the center-of-momentum frame, with the final pair at angles θ, ϕ to this axis. The helicity amplitude $M_{cd;ab}(\theta,\phi)$, where a is the helicity of particle A, etc., in a generic process $A+B \to C+D$, may be expanded:

$$M_{cd;ab}(\theta,\phi) = \sum_J (2J+1) D^{(J)*}_{\mu\mu'}(\phi,\theta,-\phi) T^J_{\mu\mu'}/4\pi , \tag{2}$$

where $\mu = a-b$, $\mu' = c-d$, $J \geq |\mu|, |\mu'|$, and

$$T^J_{\mu\mu'} \equiv \langle JM;cd|T|JM;ab\rangle \equiv \langle cd|T^J|ab\rangle , \tag{3}$$

where T^J is the transition matrix between states with angular momentum J. The $D^{(J)}_{\mu\mu'}(\alpha,\beta,\gamma)$ are the rotation matrices and α, β, and γ are the usual Euler angles. The $T^J_{\mu\mu'}$ are obtained from the helicity amplitudes by means of the integrals

$$T^J_{\mu\mu'} = \int d\Omega\, M_{cd;ab} D^{(J)}_{\mu\mu'}(\phi,\theta,-\phi) . \tag{4}$$

The selection rules that arise from considerations of charge conjugation and parity may be easily derived. A general n-gluon state is not necessarily an eigenstate of the charge-conjugation operator, but the two-gluon states that will be encountered in this paper, namely, color-singlet two-gluon states, are. The charge-conjugation eigenvalue of these states is $+1$.

For fermion-antifermion pairs the charge conjugation is $(-1)^{L+S}$. For triplet ($S=1$) fermion pairs [states $|1\rangle$, $|3\rangle$, and $|4\rangle$ in Eq. (1)], L is therefore odd. The parity of a fermion pair is $(-1)^{L+1}$, so that triplet pairs are always positive-parity states in a color-singlet, two-gluon process. Thus, the state $|3\rangle$ in Eq. (1) exists only for even J, while the state $|4\rangle$ exists only for odd J.

On the other hand, positive charge conjugation means that L is even for singlet ($S=0$) pairs [state $|2\rangle$ in Eq. (1)], so that the parity is negative. In addition, since $J=L$, and L is even, partial waves with $J^P=(2n+1)^-$ are forbidden. All other partial waves are possible.

For $q\bar{q} \to gg \to Q\bar{Q}$, the allowed transitions are

$$\begin{aligned}
&|1\rangle \to |1'\rangle \quad [(-1)^J], \quad |2\rangle \to |2'\rangle \quad [(-1)^{J+1}] ,\\
&|1\rangle \to |3'\rangle \quad [(-1)^J], \quad |3\rangle \to |3'\rangle \quad [(-1)^J] ,\\
&|3\rangle \to |1'\rangle \quad [(-1)^J], \quad |4\rangle \to |4'\rangle \quad [(-1)^{J+1}] ,
\end{aligned}$$

where the notation is the same as in Eq. (1), and the primed states are final states, while the unprimed ones are initial states. The quantities in square brackets are the parities of the states. Note that charge conjugation and parity invariance forbid singlet$\leftrightarrow$triplet transitions.

The allowed partial waves may be described in terms of the total spin and relative angular momentum of the annihilating quarks. For the negative-parity partial waves, the decomposition is

$$0^- = {}^1S_0, \quad 2^- = {}^1D_2, \quad 2n^- = {}^1(2n)_{2n} .$$

The positive-parity waves with odd J are

$$\begin{aligned}
&1^+ = -{}^3P_1, \quad 3^+ = -{}^3F_3 ,\\
&(2n+1)^+ = -{}^3(2n+1)_{2n+1} .
\end{aligned}$$

There are four contributions to the positive-parity partial waves with even J. Pairs with parallel spins give rise to the partial waves

$$\begin{aligned}
2^+ &= (\tfrac{3}{5})^{1/2}\,{}^3P_2 + (\tfrac{2}{5})^{1/2}\,{}^3F_2 ,\\
4^+ &= (\tfrac{5}{9})^{1/2}\,{}^3F_4 + (\tfrac{4}{9})^{1/2}\,{}^3H_4 ,\\
2n^+ &= [(2n+1)/(4n+1)]^{1/2}\,{}^3(2n-1)_{2n}\\
&\quad + [2n/(4n+1)]^{1/2}\,{}^3(2n+1)_{2n} .
\end{aligned} \tag{5}$$

Pairs with antiparallel spins correspond to

$$\begin{aligned}
2^+ &= (\tfrac{2}{5})^{1/2}\,{}^3P_2 - (\tfrac{3}{5})^{1/2}\,{}^3F_2 ,\\
4^+ &(\tfrac{4}{9})^{1/2}\,{}^3F_4 - (\tfrac{5}{9})^{1/2}\,{}^3H_4 ,\\
2n^+ &= [2n/(4n+1)]^{1/2}\,{}^3(2n-1)_{2n}\\
&\quad - [(2n+1)/(4n+1)]^{1/2}\,{}^3(2n+1)_{2n} .
\end{aligned} \tag{6}$$

The contributions to the positive-parity partial waves with even J from the M_{+++-}, etc., represent transitions from the first set of L-S states above [Eq. (5)], to the second set [Eq. (6)], while the contributions from the M_{+-++}, etc., represent transitions from the second set of states to the first set.

Note also that the 4×4 transition matrix, with 16 possible transition amplitudes, of which only six are independent, decouples into two 2×2 matrices, one for transitions between states with natural parity, and the other for transitions between states with unnatural parity. In the former matrix, all four transitions are independent and allowed, while in the latter, only two are allowed. This is in contrast with the particle-particle transition matrix, where each of the submatrices has three, independent, allowed amplitudes.

In concluding this section it may be pointed out that consideration of the symmetry properties of the helicity states and helicity amplitudes has led to the selection rules and enumeration of possible partial waves described above. It is now left to investigate the energy dependence of the allowed partial waves.

III. ANALYSIS

Figures 1(a) and 1(b) show the choices of momenta for the quark and gluon propagators. These are the same as those of Berends, Gaemers, and Gastmans.[7] In terms of these momenta, and ignoring a trivial color factor of $\frac{2}{3}$, the amplitude M for $q\bar{q}\to gg\to Q\bar{Q}$ is

$$iM=g^4\int\frac{d^4k}{(2\pi)^4}\frac{\bar{u}(q_-)\gamma_\alpha(\not{Q}-\not{k}+m_1)\gamma_\beta v(q_+)\bar{v}(P_+)\gamma^\beta(\not{\Delta}-\not{k}+m)\gamma^\alpha u(P_-)}{(+)(-)(\Delta)(Q)}$$
$$+g^4\int\frac{d^4k}{(2\pi)^4}\frac{\bar{u}(q_-)\gamma_\alpha(\not{Q}+\not{k}+m_1)\gamma_\beta v(q_+)\bar{v}(P_+)\gamma^\alpha(\not{\Delta}-\not{k}+m)\gamma^\beta u(P_-)}{(+)(-)(\Delta)(Q')}\,, \tag{7}$$

where

$$(\pm)=k^2\pm2k\cdot P+P^2-\lambda^2+i\epsilon,\quad (\Delta)=k^2-2k\cdot\Delta+\Delta^2-m^2+i\epsilon\,,$$
$$(Q)=k^2-2k\cdot Q+Q^2-m_1^2+i\epsilon,\quad (Q')=k^2+2k\cdot Q+Q^2-m_1^2+i\epsilon\,, \tag{8}$$

and

$$P=(P_-+P_+)/2,\quad \Delta=(P_--P_+)/2,\quad Q=(q_--q_+)/2\,.$$

λ is a gluon mass that is inserted to regularize the infrared divergences present, m is the mass of the initial quark q, and m_1 is the mass of the final quark Q. The physical significance of the gluon mass is discussed subsequently.

Let

$$M=M_a+M_b\,,$$

where

$$iM_a=g^4\int\frac{d^4k}{(2\pi)^4}\frac{\bar{u}(q_-)\gamma_\alpha(\not{Q}-\not{k}+m_1)\gamma_\beta v(q_+)\bar{v}(P_+)\gamma^\beta(\not{\Delta}-\not{k}+m)\gamma^\alpha u(P_-)}{(+)(-)(\Delta)(Q)}$$

is the contribution from Fig. 1(a) and

$$iM_b=g^4\int\frac{d^4k}{(2\pi)^4}\frac{\bar{u}(q_-)\gamma_\alpha(\not{Q}+\not{k}+m_1)\gamma_\beta v(q_+)\bar{v}(P_+)\gamma^\alpha(\not{\Delta}-\not{k}+m)\gamma^\beta u(P_-)}{(+)(-)(\Delta)(Q')}$$

is the contribution from Fig. 1(b). In the case of M_a, Feynman integrals of the type

$$(I;I_\mu;I_{\mu\nu})=\int\frac{d^4k}{(2\pi)^4}\frac{(1;k_\mu;k_\mu k_\nu)}{(+)(-)(\Delta)(Q)} \tag{9}$$

are encountered and these are evaluated in Appendix A. For M_b, the replacement $Q-k\to Q+k$ must be made.

For convenience it is simplest to work in the center-of-momentum frame. Let the $q\bar{q}$ pair travel along the z axis, with the quark having momentum $\mathbf{P}_-=P\hat{\mathbf{z}}$. The direction of motion of the $Q\bar{Q}$ pair is assumed to be at some angle θ to this axis. Any azimuthal dependence in the helicity amplitudes is trivial and is thus ignored from the outset by choosing the azimuthal angle ϕ to be zero. The momentum of Q is chosen to be

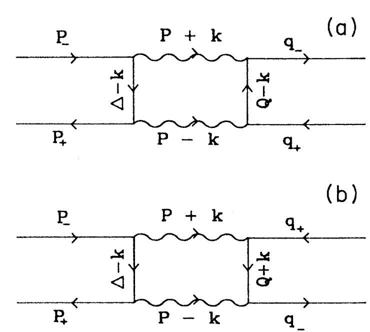

FIG. 1. (a) Uncrossed box diagram for color-singlet quark-pair annihilation. (b) Crossed box diagram for color-singlet quark-pair annihilation.

$$\mathbf{q}_{-}=P_1(\sin\theta\hat{\mathbf{x}}+\cos\theta\hat{\mathbf{z}}) .$$

Symmetries of the scattering matrix reduce from 16 to 6 the number of helicity amplitudes that must be calculated.[6] These are given in Appendix B, in terms of the Feynman integrals of Appendix A.

As written, these helicity amplitudes are quite general, and are valid for all quark masses and all energies. Some special cases that are of interest are discussed later. At this point, however, the subject of the gluon mass must be discussed.

The presence of the gluon mass λ is well understood analytically. The diagrams of Fig. 1 lead to Feynman integrals that are infrared divergent, and such a mass is needed to regularize the integrals. For the purposes of numerical calculation, this mass is kept, in the guise of a "confinement" mass. Note that the results obtained using a confinement mass are very similar to those that would be obtained using gluon brehmsstrahlung, as a similar QED calculation indicates.[8] The choice of prescription for removal of the infrared divergences has little effect on the results, and thus appears to be but a matter of taste and convenience.

A comment must be made here about comparing the results obtained with the use of a "massive" gluon, with those that would be obtained with truly massive bosons, such as W's and Z's. In arriving at the results that are presented, λ, the gluon confinement mass, is set to zero wherever possible. Thus, terms proportional to positive powers of λ, such as λ^2, are neglected. In contrast, in the case of bosons such as W's and Z's, such terms are the leading-order contributions and cannot be ignored. Comparisons between the two kinds of calculation should thus be made very carefully.

Before proceeding to describe the results of the calculation, the question of quark masses must be addressed. In this paper, only general results are presented, and these results are expected to "scale" with quark masses and energies. In all of the results that are presented, the total energy of the system exceeds 2 GeV, and the heavier quark's mass is 1 GeV. This is sufficient to illustrate the main features of the results.

IV. RESULTS FOR MASSLESS QUARKS

The general results for the helicity amplitudes, as written in Appendix B, are not very transparent. In a few limiting cases, however, the expressions become quite simple. This section deals with one of these limits, namely, the limit of massless quarks. In the next section, threshold effects when one quark mass is negligible are discussed. In addition, some results for more general cases are presented.

In the limit of massless quarks, there are only two independent helicity amplitudes, which are

$$\begin{aligned}
iM_{+-+-}&=\frac{ig^4}{4\pi^2(1+\cos\theta)}\left[\cos\theta\ln^2\frac{1-\cos\theta}{2}-(1+\cos\theta)\ln\frac{1-\cos\theta}{2}+(1+\cos\theta)^2\ln\frac{s}{\lambda^2}\ln\frac{1-\cos\theta}{1+\cos\theta}\right]\\
&\quad-\frac{g^4}{4\pi(1+\cos\theta)}\left[(1+\cos^2\theta)\ln\frac{1-\cos\theta}{1+\cos\theta}+(1+\cos\theta)+2\cos\theta\ln\frac{2}{1+\cos\theta}\right],\\
iM_{+--+}&=\frac{-ig^4}{4\pi^2(1-\cos\theta)}\left[\cos\theta\ln^2\frac{1+\cos\theta}{2}+(1-\cos\theta)\ln\frac{1+\cos\theta}{2}+(1-\cos\theta)^2\ln\frac{s}{\lambda^2}\ln\frac{1-\cos\theta}{1+\cos\theta}\right]\\
&\quad-\frac{g^4}{4\pi(1-\cos\theta)}\left[(1+\cos^2\theta)\ln\frac{1-\cos\theta}{1+\cos\theta}-(1-\cos\theta)+2\cos\theta\ln\frac{2}{1-\cos\theta}\right].
\end{aligned}\tag{10}$$

λ is the gluon mass. These results are also valid for massive quarks, but only for $\sin^2\theta\gg m^2/E^2$, where m is the mass of the heavier quark.

The unpolarized differential cross section is easily obtained from the above two amplitudes, and is shown in Fig. 2 for three energies. The total unpolarized cross section is

$$\sigma=\pi^2\alpha_s^4\left[[8\pi^2/9-16\,\mathrm{Li}_3(1)+38/3]/8\pi^2+\left[152-96\,\mathrm{Li}_5(1)+(16\pi^2/9+16/3)\ln^2\frac{s}{\lambda^2}-(40+8\pi^2/3)\ln\frac{s}{\lambda^2}\right]\Big/16\pi^4\right]\Big/E^2 \tag{11}$$

and is shown in Fig. 3. Note that $\mathrm{Li}_n(1)=\zeta(n)$, the Riemann ζ function. The form of α_s used is[9]

$$\alpha_s=12\pi/[(33-2n_q)\ln(E^2/\Lambda^2)]$$

with $n_q=6$ and $\Lambda=0.2$ GeV. This is the form used for all the results presented. The various quark thresholds have been ignored.

In obtaining Eq. (11), repeated use was made of the identity[10]

$$\mathrm{Li}_n(z)=\mathrm{Li}_n(1)+\ln(z)\mathrm{Li}_{n-1}(z)-\ln^2(z)\mathrm{Li}_{n-2}(z)/2!+\ln^3(z)\mathrm{Li}_{n-3}(z)/3!$$
$$-\cdots+(-1)^{n-1}\ln^{n-2}(z)\mathrm{Li}_2(z)/(n-2))!+(-1)^{n-1}\ln^{n-1}(z)\ln(1-z)/(n-1)!$$
$$+(-1)^{n-1}\int_1^z dz[\ln^{n-1}(z)]/[(1-z)(n-1)!]\ , \tag{12}$$

where

$$\mathrm{Li}_n(x)=\int_0^x dz\ \mathrm{Li}_{n-1}(z)/z$$

is the polylogarithm function, with

$$\mathrm{Li}_2(x)=-\int_0^x dz\ \ln(1-z)/z\ .$$

The massless quark case is one of a few cases in which the total unpolarized cross section can be calculated analytically. A second case is near threshold when one quark mass is negligible. In most other limits, the cross section must be evaluated numerically.

The partial-wave amplitudes for $J\le 4$ are

$$iT^1_{11}=ig^4(3-2Z)/2\pi\ ,$$
$$iT^2_{11}=2ig^4(10-9Z)/27\pi+4g^4/9\ ,$$
$$iT^3_{11}=ig^4(361-144Z)/864\pi+5g^4/72\ , \tag{13}$$
$$iT^4_{11}=ig^4(9771-4400Z)/36\,000\pi+121g^4/1800\ ,$$
$$Z=\ln\frac{s}{\lambda^2}\ .$$

The above amplitudes arise from M_{+-+-}. The amplitudes arising from M_{+--+} are the same as those above within a factor of ± 1. The imaginary parts of the above partial-wave amplitudes are obtained from the partial-wave amplitudes for $q\bar{q}\to gg$ and $gg\to q\bar{q}$ via the unitarity condition. These are given in Appendix C for the general case. The partial-wave cross sections for $J\le 4$ are

$$\sigma^{1^+}=3\alpha_s^4(3-2Z)^2/(4\pi E^2)\ ,$$
$$\sigma^{2^+}=5\pi\alpha_s^4[4(10-9Z)^2/(729\pi^2)+16/81]/E^2\ , \tag{14}$$
$$\sigma^{3^+}=7\pi\alpha_s^4[(361-144Z)^2/(746\,496\pi^2)+25/5184]/E^2\ ,$$
$$\sigma^{4^+}=9\pi\alpha_s^4[(9771-4400Z)^2/(1.296\times 10^9\pi^2)+14\,641/3\,240\,000]/E^2\ .$$

These partial-wave cross sections are shown in Fig. 3 for a range of energy between 1 and 100 GeV, for $\lambda=0.3$ GeV. The total unpolarized cross section is also shown. Figure 4 shows the same cross sections, but with $\lambda=0.6$ GeV. The negative-parity partial waves vanish in this limit since the amplitudes that lead to such partial waves are proportional to the quark masses. For the same reason, the 0^+ partial wave also vanishes in the limit of massless quarks.

V. GENERAL FEATURES AND THRESHOLD EFFECTS

The general features for the total, partial-wave, and differential cross sections for massive quark-pair transmutation are best discussed in three different cases: light quarks→heavy, heavy→light, and the case when all the quark masses are the same. In all cases, the mass of the heavier quark is chosen to be 1 GeV.

Figures 5–7 show the differential cross sections for the case when a light pair is transformed into a heavy pair. In all of these cases are shown the unpolarized differential cross section, as well as the angular distributions arising from singlet and triplet quark pairs.

In Fig. 5, the energy is just beyond the threshold for the creation of the final-state pair ($m=0.7$ GeV, $m_1=1$

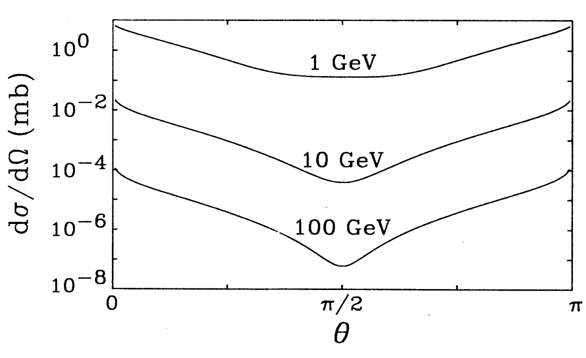

FIG. 2. Angular distribution from massless quarks.

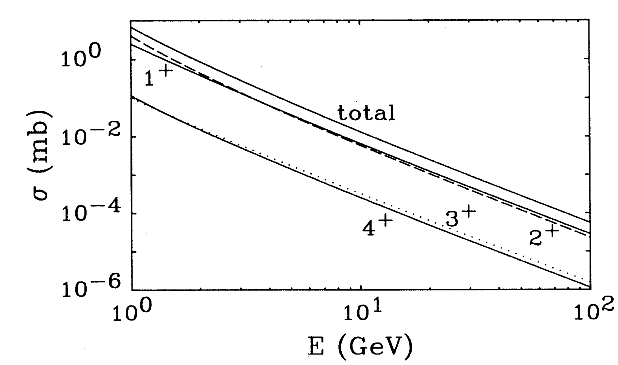

FIG. 3. Partial-wave and total cross sections for massless quarks, $\lambda=0.3$ GeV.

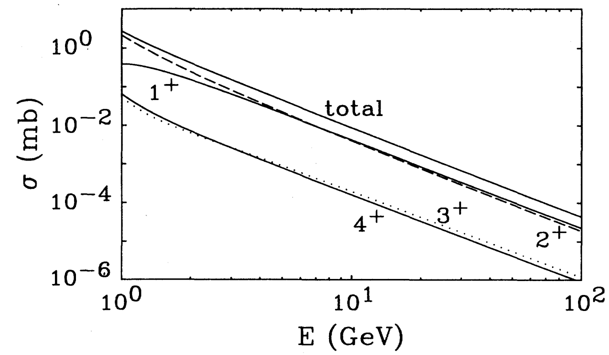

FIG. 4. Partial-wave and total cross sections for massless quarks, $\lambda=0.6$ GeV.

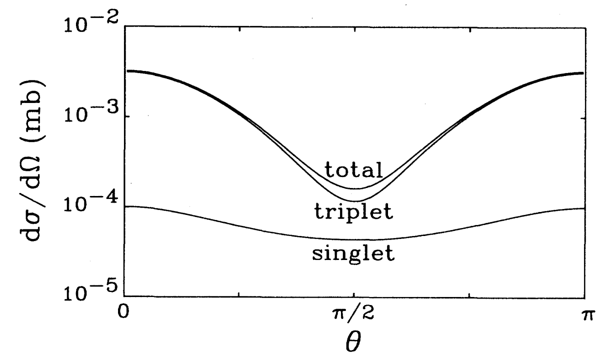

FIG. 6. Angular distributions for light$\rightarrow$heavy, intermediate energy.

GeV, $E=1.001$ GeV). This pair is expected to be produced in the partial wave 0^-; S-wave spin-singlet state. The isotropic distribution clearly shows S-wave annihilation.

In Fig. 6, the energy is intermediate ($E=2$ GeV), and the increased proportion of triplet annihilation is clear. In Fig. 7, the energy of the final pair is much larger than their mass ($E=20$ GeV) and triplet annihilation and production dominate. The triplet distribution in Fig. 7 is indistinguishable from the unpolarized cross section on the scale used.

A comment must be made about the comparison between Fig. 2, which shows the differential cross section for massless quarks, and Fig. 7, which shows the angular distribution for massive quarks at high energy. The difference between the two sets of curves is not very striking, except in the forward and backward directions. Massive quarks lead to a forward peaked distribution, but not as peaked as for massless quarks.

The forward peak for massive quarks at high energy is in fact finite, and has been found to be independent of θ, the scattering angle, to leading order for small θ. In contrast, the forward differential cross section for massless quarks is proportional to various powers of $\ln\theta$, the highest being $\ln^4\theta$, as is evident from Eq. (10).

Figure 8 shows the total unpolarized cross sections, as well as the cross sections arising from singlet and triplet pairs. The dominance of triplet production at high energies and singlet production near threshold are clearly seen. These cross sections were evaluated using 96 point Gaussian quadrature methods.

Note that near threshold, for quark pairs of differing mass, there is "competition" between singlet and triplet production. Near threshold, for pairs with very different masses, the light-pair annihilation is triplet dominated, while the heavy-pair production is singlet dominated. From the selection rules of Sec. II, a triplet to singlet transition is forbidden, so that which mode of annihilation dominates depends on how different the quark masses are and on how close to threshold the energy is. In Fig. 8, the ratio of masses is 0.7. Figures 9 and 10 illustrate the effect of the differing mass ratios.

The threshold behavior of the cross sections is understood by expanding the helicity amplitudes in powers of v_1, the magnitude of the center-of-momentum velocity of the final-state quarks. This is most easily done when $v \sim 1 (m \sim 0)$. Then, only two helicity amplitudes contribute, and they are

$$iM_{++++} = -iM_{++--} = imm_1\left[2\ln\frac{2}{1-v} - \tfrac{1}{2}\ln^2\frac{2}{1-v} - \pi^2/6\right]\Big/(8\pi^2E^2) + mm_1\left[\ln\frac{2}{1-v}\right]\Big/(8\pi E^2) . \tag{15}$$

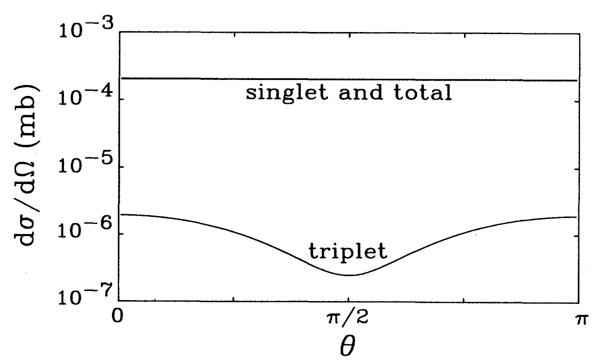

FIG. 5. Angular distributions for light quarks$\rightarrow$heavy near threshold.

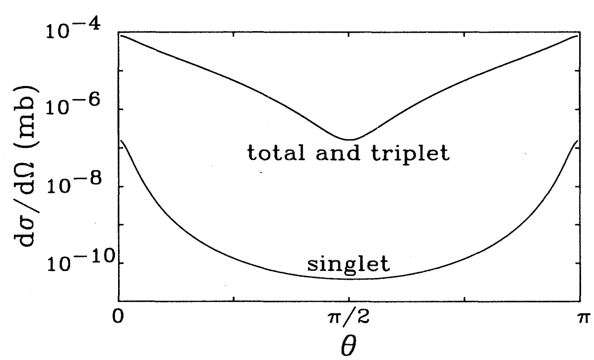

FIG. 7. Angular distribution for light$\rightarrow$heavy, high energy.

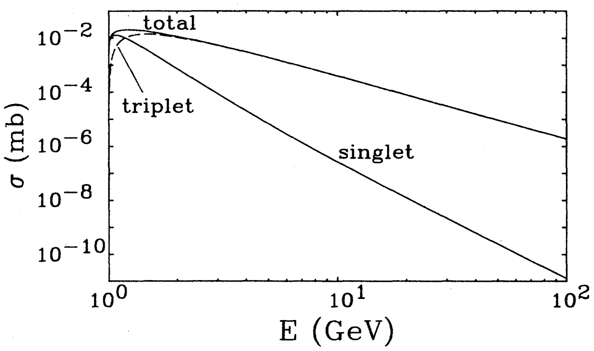

FIG. 8. Total cross sections, light→heavy, $m/m_1=0.7$.

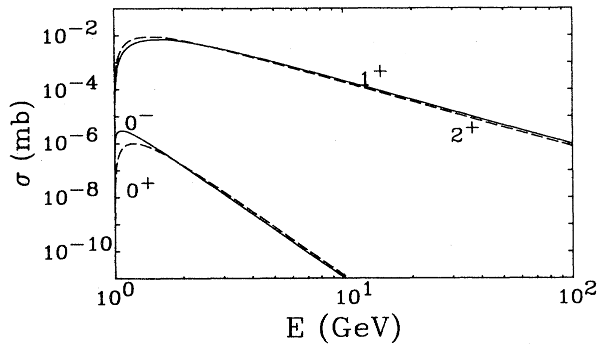

FIG. 10. Partial-wave cross sections, light→heavy, $m/m_1=0.001$.

These are independent of v_1, and finally lead to cross sections that are proportional to v_1 when the phase-space factors are included. The triplet helicity amplitudes are all proportional to higher powers of v_1. The v_1 dependence of the cross section means that for the case of light→heavy, the cross sections rise from zero near threshold and increase linearly with v_1 in the case of singlet annihilation. Note that even though the triplet cross sections are proportional to higher powers of v_1 near threshold, terms similar to the logarithmic ones in Eq. (15) can still make the triplet cross sections quite large if v is sufficiently close to unity.

The dominant partial-wave cross sections for the case light→heavy are shown in Figs. 9 and 10. In Fig. 9, the ratio of quark masses is 0.7, while in Fig. 10 it is 0.001. 0^- is the dominant partial wave near threshold in the former figure, while in the latter, the 2^+ partial wave very quickly becomes dominant. This is another manifestation of the competition between singlet and triplet production near threshold, mentioned above.

The cross sections for heavy→light are shown in Fig. 11. The major differences between these curves and those of Fig. 8 are observed when the annihilating pair are nearly at rest. Again, singlet annihilation dominates (depending on the quark mass ratio), and the cross section is now proportional to $1/v$, where v is the velocity of the initial pair. This is well understood as being a result of the principle of detailed balance:[11] the cross sections for heavy→light and light→heavy near threshold are related by a factor of v^2, where v is the velocity of the heavy quark.

The case when all the quarks have the same mass is special near threshold. Here, the amplitudes near threshold are independent of velocities, as in all the other cases. In evaluating a cross section, phase space introduces a factor of v_1/v. For quarks of equal masses, $v_1=v$, and the cross sections near threshold are completely independent of velocities. Figure 12 illustrates this for the total cross section. Note that, in this case, there can be no competition between singlet and triplet annihilation near threshold, so that singlet annihilation clearly dominates.

All of the results so far described have been obtained with a gluon mass of 0.3 GeV. Figure 13 shows typical results for the partial-wave cross sections, obtained with

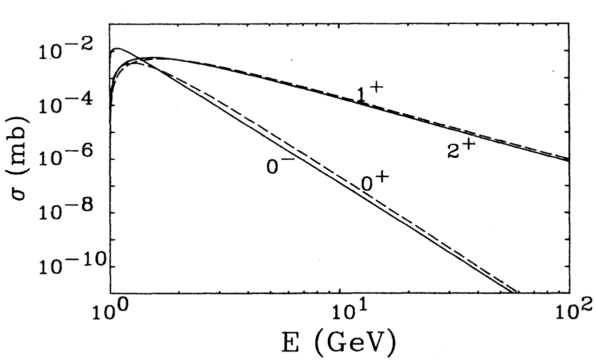

FIG. 9. Partial-wave cross sections, light→heavy, $m/m_1=0.7$.

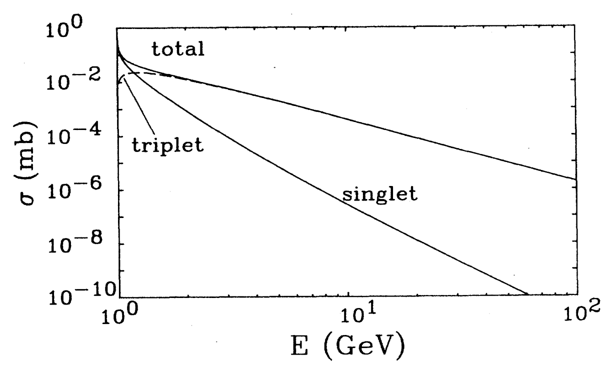

FIG. 11. Total cross sections, heavy→light.

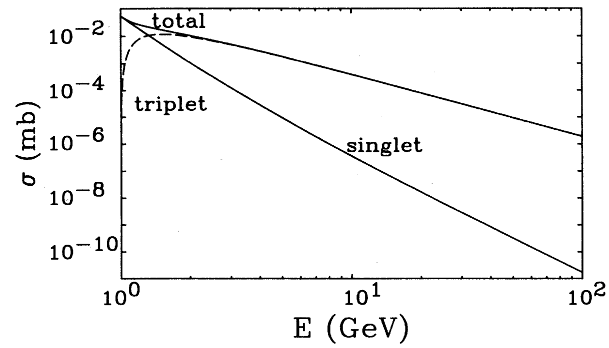

FIG. 12. Total cross sections, $m = m_1$.

a gluon mass of 0.6 GeV. Note that singlet annihilation is completely independent of λ; the terms dependent on λ disappear when the appropriate helicity amplitudes are combined to obtain the singlet$\rightarrow$singlet transition amplitude. As a result, the partial-wave cross sections for production of negative-parity partial waves are also independent of λ. Note, however, that the 0^+ partial wave is sensitive to λ. In addition, all of the cross sections are independent of λ near threshold.

In closing this section, a comment will be made about the validity of applying the partial-wave cross sections obtained for massless quarks to generally massive quarks. One method of testing this validity is by investigating the energy dependence of the ratio of the partial-wave cross sections for massive quarks to the corresponding partial-wave cross sections for massless quarks.

This is shown in Fig. 14 for the 2^+ partial wave. Within 10%, the asymptotic expression for the 2^+ partial wave is seen to be valid for energies greater than about ten times the mass of the heavier quark. Within 1%, this number increases to about 15 to 20 times the heavy-quark mass. For many applications, it appears that the very simple asymptotic forms of the partial-wave and total cross sections, as shown in Eqs. (11) and (14), will suffice.

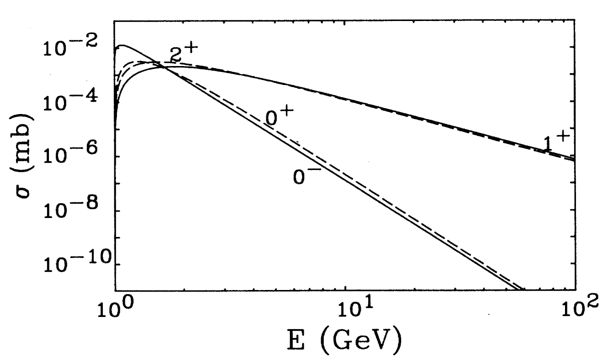

FIG. 13. Partial-wave cross sections, light$\rightarrow$heavy, $\lambda=0.6$ GeV.

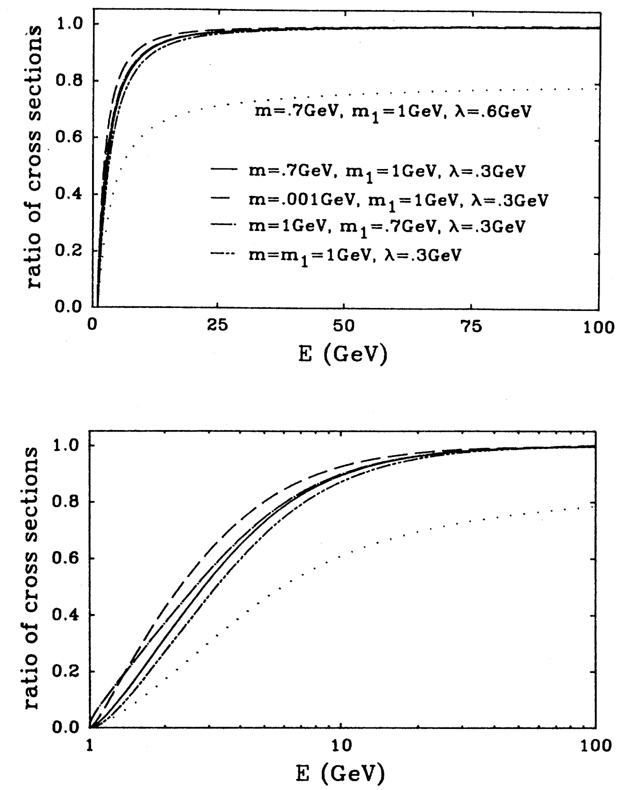

FIG. 14. Comparison of partial-wave cross section with asymptotic limit for 2^+ partial wave.

VI. SUMMARY

In QCD, quark-pair transmutation *via* a two-gluon intermediate state shows many features that are similar to those seen in quark-pair annihilation *into* two gluons:[12,13] triplet annihilation dominates at energies large compared with all quark masses, while singlet annihilation tends to dominant near threshold. The triplet contribution is dominated by pairs with parallel spins. However, there is competition between triplet annihilation of a light pair, say, and singlet production of a heavy pair near threshold. The dominant mode of annihilation depends on the ratio of quark masses and on how close to threshold the energy actually is.

In terms of partial waves, the results here are essentially the same as those obtained for pair annihilation into two gluons, except for the appearance of a new partial wave. This new partial wave 1^+ turns out to be the marginally dominant one at high energies. The asymptotic forms obtained for the partial wave and total cross sections are valid, to within about 10%, for energies greater than about ten times the mass of the heavier quark.

At high energies, transmutation from pairs with spins parallel clearly dominates in any pair annihilation process and is a result of the γ_μ couplings. The level of the dominance of this mode of annihilation over annihilation from pairs with spins antiparallel is easily estimated.

For each pair involved, the cross section from pairs with spins antiparallel is suppressed by a factor of m^2/E^2 compared with the cross section from pairs with parallel spins. Thus, in $q\bar{q} \rightarrow Q\bar{Q}$, the ratio of cross sections is roughly 1: m^2/E^2: m^4/E^4, where the 1 corresponds to pairs with spins parallel annihilating into pairs with spins parallel, the m^2/E^2 corresponds to either the initial or final pair having spins antiparallel, and the m^4/E^4 corresponds to both pairs having spins antiparallel.

In concluding this section, it must be pointed out that although the unitarity condition was very useful in calculating most of the partial waves, it does not predict any 1^+ partial wave, nor does it forbid it. Via this condition, all the other partial-wave cross sections could be estimated very roughly from the real parts of the partial-wave amplitude obtained from the lower-order processes. However, new partial waves, the amplitudes of which possess no real part, are still possible.

To understand how this can come about, it is necessary to trace the steps in evaluating the full amplitude from the unitarity condition. In the scattering matrix, the imaginary part of the amplitude can be obtained from the amplitudes for lower-order processes via the unitarity condition. For the case at hand, this forbids the 1^+ partial wave for massless gauge bosons.

The full amplitude is then obtained from this imaginary part by means of a dispersion relation. From the form of the imaginary part of the amplitude at high energies, a once subtracted dispersion relation is needed.[6] Note, however, that only the helicity amplitudes such as M_{+-+-}, etc., need the subtraction term. While the dispersion integrals that arise do not give rise to a 1^+ partial wave, the subtraction term can. In keeping with this, the helicity amplitudes M_{+-+-}, etc., are the only ones that contribute to the 1^+ partial wave. For a general process, such subtraction terms can give rise to partial-wave amplitudes whose imaginary parts vanish in accordance with the unitarity condition.

Note that there are two deficiencies introduced by approximating a process such as $q\bar{q} \rightarrow gg \rightarrow Q\bar{Q}$ by the "cut" process $q\bar{q} \rightarrow gg$, as illustrated in Fig. 15. The first is the observation that not all possible partial waves will necessarily be represented by the cut process. Thus, for instance, the commonly held belief that a $^3P_1$ quarkonium state will not decay via a two-gluon or two-photon intermediate state[14] is clearly incorrect, as the results of Secs. IV and V have shown.

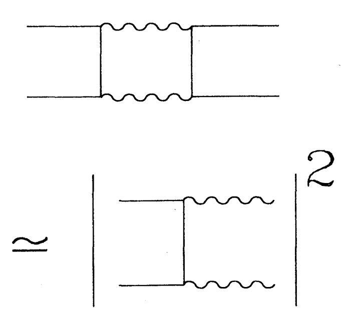

FIG. 15. "Uncut" and "cut" two-gluon quark-pair annihilation.

The second deficiency becomes apparent when the infrared behavior of cut amplitudes and cross sections are investigated. For $q\bar{q} \rightarrow gg$, there is no divergence which results from the massless nature of the gluons. For the full, uncut process, however, there is such a divergence, and the physical and perhaps philosophical problems presented by this are simply nonexistent in the cut process approximation.

VII. FUTURE WORK AND CONCLUDING REMARKS

The work described in this paper can be extended in many directions, and can be applied to a number of different processes. In this section, some ideas for such future work will be briefly described.

One obvious application of the results is to the OZI-suppressed decays of quarkonia. With the helicity amplitudes evaluated, any spin effects in the decays can be easily taken into account. Such an application assumes, of course, that the decay proceeds via two-gluon annihilation.

As hinted at in Sec. I, the results obtained may be used in formulating a model for quark-pair production. For light or massless quarks, this would have to be a "$^3P_1$" or "$^3P_2$" model, in contrast with the $^3P_0$ and $^3S_1$ models that are popular at present. Note, however, that any model developed would allow many other possible partial waves. For light quarks, for instance, not only would $^3P_1$ and $^3P_2$ be allowed, but so would $^3F_2$, $^3F_3$, $^3F_4$, and $^3H_4$, to name just a few. For quark pairs produced near their pair-creation threshold, the allowed partial waves would include $^1S_0$, $^1D_2$, and $^3P_0$.

The development of such a model is quite important for particle phenomenology, as the two existing models are somewhat inadequate on some points. As mentioned earlier, both the $^3P_0$ and $^3S_1$ models allow only one partial wave for pair production, and as such they are somewhat restrictive. For instance, neither model can be used to describe the OZI-suppressed decay of quarkonia with quantum numbers of 1^+ or 0^-, say. Note that although a model based on the results of this work will allow quark pairs to be produced with quantum numbers corresponding to $^3P_0$, this partial wave is never a dominant one.

The amplitudes obtained here could also find uses in other aspects of particle spectroscopy. Mixing between mesons such as η and η' may be estimated from them. The validity of such a calculation obviously hinges on the assumption that perturbative QCD is correct at the energies concerned.

More exotic applications of these results can obviously be found. One particular process to which they may be immediately applicable is to the glueball production reaction[15] $\pi^- p \rightarrow \phi\phi n$. Previously, this process was investigated by Karl, Roberts, and Zagury,[16] which provided part of the original motivation for this work. A more recent study has already been undertaken by Roberts and Karl.[17] This new study includes the pair-transmutation description of this paper.

ACKNOWLEDGMENTS

The author acknowledges many useful and enlightening discussions with Dr. Gabriel Karl during the completion of this work. Conversations with Dr. Peter Zencyzkowski, Dr. George Leibbrandt, and Dr. Bernhard Nickel have also been helpful. This research was funded in part by the Government of Ontario and by the Natural Sciences and Engineering Research Council of Canada.

APPENDIX A: FEYNMAN INTEGRALS

The Feynman integrals encountered are

$$(I;I_\mu;I_{\mu\nu})=\int\frac{d^4k}{(2\pi)^4}\frac{(1;k_\mu;k_{\mu\nu})}{(+)(-)(\Delta)(Q)}\ ,$$

which are expressible in terms of the relatively simpler integrals

$$F=\int\frac{d^4k}{(2\pi)^4}\frac{1}{(-)(\Delta)(Q)}=\int\frac{d^4k}{(2\pi)^4}\frac{1}{(+)(\Delta)(Q)}\ ,$$

$$G=\int\frac{d^4k}{(2\pi)^4}\frac{1}{(+)(-)(Q)},\quad H=\int\frac{d^4k}{(2\pi)^4}\frac{1}{(+)(-)(\Delta)}\ ,$$

$$L=\int\frac{d^4k}{(2\pi)^4}\frac{1}{(-)(\Delta)}=\int\frac{d^4k}{(2\pi)^4}\frac{1}{(+)(\Delta)}\ ,$$

$$N=\int\frac{d^4k}{(2\pi)^4}\frac{1}{(-)(Q)}=\int\frac{d^4k}{(2\pi)^4}\frac{1}{(+)(Q)}\ ,$$

$$R=\int\frac{d^4k}{(2\pi)^4}\frac{1}{(\Delta)(Q)},\quad S=\int\frac{d^4k}{(2\pi)^4}\frac{1}{(+)(-)}\ .$$

In the above,

$$(\pm)=k^2\pm 2k\cdot P+E^2-\lambda^2+i\epsilon\ ,$$

$$(\Delta)=k^2-2k\cdot\Delta-E^2+i\epsilon\ ,$$

$$(Q)=k^2-2k\cdot Q-E^2+i\epsilon\ ,$$

where P, Δ, and Q are as defined in Eq. (8). The integrals I and F to S are evaluated with the use of Feynman parametrization and dimensional regularization.[18–21]

The results for these integrals are

$$I=\frac{i}{256\pi^2E^2\Phi}\ln\frac{E^2-PP_1\cos\theta-\Phi}{E^2-PP_1\cos\theta+\Phi}\left[2\ln\frac{s}{\lambda^2}-i\pi\right]\ ,$$

where

$$\Phi=[E^2(P^2+P_1^2)-P^2P_1^2(1-\cos^2\theta)-2E^2PP_1\cos\theta]^{1/2}=[-E^2t-P^2P_1^2(1-\cos^2\theta)]^{1/2}\ ,$$

$$\begin{aligned}F=\frac{i}{64\pi^2\Phi}\Bigg[&\ln\frac{E^2-PP_1\cos\theta-\Phi}{E^2-PP_1\cos\theta+\Phi}\ln\frac{2\Phi}{\lambda^2}\\&+\tfrac{1}{2}\ln\left|\frac{(P^2-PP_1\cos\theta-\Phi)(P_1^2-PP_1\cos\theta+\Phi)}{t^2}\right|\ln\left|\frac{P^2-PP_1\cos\theta-\Phi}{P_1^2-PP_1\cos\theta+\Phi}\right|\\&+\tfrac{1}{2}\ln\left|\frac{(P_1^2-PP_1\cos\theta-\Phi)(P^2-PP_1\cos\theta+\Phi)}{t^2}\right|\ln\left|\frac{P_1^2-PP_1\cos\theta-\Phi}{P^2-PP_1\cos\theta+\Phi}\right|\\&+\mathrm{Li}_2\frac{P^2-PP_1\cos\theta+\Phi}{2\Phi}+\mathrm{Li}_2\frac{P_1^2-PP_1\cos\theta+\Phi}{2\Phi}\\&-\mathrm{Li}_2\frac{P^2-PP_1\cos\theta-\Phi}{-2\Phi}-\mathrm{Li}_2\frac{P_1^2-PP_1\cos\theta-\Phi}{-2\Phi}\Bigg]\ ,\end{aligned}$$

$$\begin{aligned}&G=\frac{i}{64\pi^2E^2v_1}\left[\mathrm{Li}_2\frac{v_1-1}{1+v_1}-\mathrm{Li}_2\frac{1+v_1}{v_1-1}-i\pi\ln\frac{1+v_1}{1-v_1}\right],\quad H=\frac{i}{64\pi^2E^2v}\left[\mathrm{Li}_2\frac{v-1}{1+v}-\mathrm{Li}_2\frac{1+v}{v-1}-i\pi\ln\frac{1+v}{1-v}\right]\ ,\\&L=\frac{i\Gamma(\delta)}{16\pi^2\mu^{2\delta}}\{1+\delta[\ln(\mu^2/m^2)+2-i\pi]\},\quad N=\frac{i\Gamma(\delta)}{16\pi^2\mu^{2\delta}}\{1+\delta[\ln(\mu^2/m_1^2)+2-i\pi]\}\ ,\\&S=\frac{i\Gamma(\delta)}{16\pi^2\mu^{2\delta}}\{1+\delta[\ln(\mu^2/s)+2]\}\ ,\end{aligned}\tag{A1}$$

$$R=\frac{i\Gamma(\delta)}{16\pi^2\mu^{2\delta}}\left[1+\delta\left[\ln(\mu^2/m^2)+\frac{P_1^2-PP_1\cos\theta}{t}\ln\frac{m_1^2}{m^2}+\frac{\Phi}{t}\ln\frac{E^2-PP_1\cos\theta+\Phi}{E^2-PP_1\cos\theta-\Phi}+2-i\pi\right]\right]\ .$$

In the above, $v = P_\pm/E$, $v_1 = P_1/E$, and $\delta = (4-n)/2$, where n is the dimension of space-time. μ is a mass that is inserted to make the integrals dimensionally correct. The final results are independent of μ and δ.

$$\mathrm{Li}_2(x) = -\int_0^x dz[\ln(1-z)]/z$$

is the dilogarithm function.

The integral I_μ is readily evaluated in terms of the simpler integrals above by means of the ansatz

$$I_\mu = \beta_1 \Delta_\mu + \gamma_1 Q_\mu \ . \tag{A2}$$

Taking the four-vector dot product of this equation with Δ^μ and Q^μ, respectively, leads to the pair of simultaneous equations

$$-P^2\beta_1 - PP_1\cos\theta\gamma_1 = (F - G - 2E^2 I)/2 \ , \tag{A3}$$

$$-PP_1\cos\theta\beta_1 - P_1^2\gamma_1 = (F - H - 2E^2 I)/2 \ , \tag{A4}$$

the solutions of which are

$$\beta_1 = \frac{(P_1^2 - PP_1\cos\theta)(2E^2 I - F) + P_1^2 G - PP_1\cos\theta H}{2P^2P_1^2(1-\cos^2\theta)} \ , \tag{A5}$$

$$\gamma_1 = \frac{(P^2 - PP_1\cos\theta)(2E^2 I - F) + P^2 H - PP_1\cos\theta G}{2P^2P_1^2(1-\cos^2\theta)} \ . \tag{A6}$$

Note that I_μ is independent of P_μ.

A similar procedure leads to the decomposition

$$I_{\mu\nu} = a_1 P_\mu P_\nu + b_2 \Delta_\mu \Delta_\nu + c_2 Q_\mu Q_\nu + c_3(Q_\mu \Delta_\nu + \Delta_\mu Q_\nu) + \epsilon g_{\mu\nu} \ , \tag{A7}$$

where

$$a_1 = -\{4E^4 I[-E^2 t - P^2P_1^2(1-\cos^2\theta)] - E^2 t(R - 2E^2 F) - E^2(N - 2E^2 G)(P_1^2 - PP_1\cos\theta) - E^2(L - 2E^2 H)(P^2 - PP_1\cos\theta) + 2X[-E^2 t - 2P^2P_1^2(1-\cos^2\theta)]\}/[4E^4P^2P_1^2(1-\cos^2\theta)] \ , \tag{A8}$$

$$b_2 = \{2[X + E^2(2E^2 I - F)][-2E^2 t - P^2(E^2 + P_1^2)(1-\cos^2\theta)] - 2E^2(N - 2E^2 G)(P_1^2 - PP_1\cos\theta) + E^2(L - 2E^2 H)[PP_1\cos\theta(3-\cos^2\theta) - P^2(1+\cos^2\theta)] + E^2 R[-2t - P^2(1-\cos^2\theta)] - E^2 PP_1\cos\theta(1-\cos^2\theta)S\}/[4E^2P^4P_1^2(1-\cos^2\theta)^2] \ , \tag{A9}$$

$$c_2 = \{2[X + E^2(2E^2 I - F)][2E^2 t\cos\theta + PP_1(E^2 + PP_1\cos\theta)(1-\cos^2\theta)] + E^2(N - 2E^2 G)[2P_1^2\cos\theta - PP_1(1+\cos^2\theta)] + E^2(L - 2E^2 H)[2P^2\cos\theta - PP_1(1+\cos^2\theta)] + E^2 R[2t\cos\theta + PP_1(1-\cos^2\theta)] + E^2 PP_1(1-\cos^2\theta)S\}/[4E^4P^3P_1^3(1-\cos^2\theta)^2] \ , \tag{A10}$$

$$c_3 = \{2[X + E^2(2E^2 I - F)][-2E^2 t - P_1^2(E^2 + P^2)(1-\cos^2\theta)] - 2E^2(L - 2E^2 H)(P^2 - PP_1\cos\theta) + E^2(N - 2E^2 G)[PP_1\cos\theta(3-\cos^2\theta) - P_1^2(1+\cos^2\theta)] + E^2 R[-2t - P_1^2(1-\cos^2\theta)] - E^2 PP_1\cos\theta(1-\cos^2\theta)S\}/[4E^2P^2P_1^4(1-\cos^2\theta)^2] \ , \tag{A11}$$

$$\epsilon = -\{2[X + E^2(2E^2 I - F)][E^2 t + P^2P_1^2(1-\cos^2\theta)] + E^2 tR + E^2(N - 2E^2 G)(P_1^2 - PP_1\cos\theta) + E^2(L - 2E^2 H)(P^2 - PP_1\cos\theta)\}/[4E^2P^2P_1^2(1-\cos^2\theta)] \ . \tag{A12}$$

$I_{\mu\nu}$ is independent of terms linear in P_μ. The coefficients β_1, γ_1, a_1, b_2, c_2, c_3, and ϵ are the same as those of Berends, Gaemers, and Gastmans[7] (I_Δ, I_Q, K_P, K_Δ, K_Q, K_X, and K_0, respectively). The quantity X is given by

$$X = \frac{i}{64\pi^2 E^2 \Phi} \ln \frac{E^2 - PP_1\cos\theta - \Phi}{E^2 - PP_1\cos\theta + \Phi} \ . \tag{A13}$$

APPENDIX B: HELICITY AMPLITUDES

The amplitude for the process $q\bar{q} \to gg \to Q\bar{Q}$, ignoring color factors, is given in terms of the Feynman integrals of Appendix A as

$$\begin{aligned} iM = {} & g^4 \bar{u}(q_-)\gamma_\alpha\gamma^\rho\gamma_\beta v(q_+)\bar{v}(P_+)\gamma^\beta\gamma^\lambda\gamma^\alpha u(P_-)(Q_\rho\Delta_\lambda I - I_\rho\Delta_\lambda - Q_\rho I_\lambda + I_{\rho\lambda}) \\ & + m_1 g^4 \bar{u}(q_-)\gamma_\alpha\gamma_\beta v(q_+)\bar{v}(P_+)\gamma^\beta\gamma^\lambda\gamma^\alpha u(P_-)(\Delta_\lambda I - I_\lambda) \\ & + m g^4 \bar{u}(q_-)\gamma_\alpha\gamma^\rho\gamma_\beta v(q_+)\bar{v}(P_+)\gamma^\beta\gamma^\alpha u(P_-)(Q_\rho I - I_\rho) \\ & + m m_1 g^4 \bar{u}(q_-)\gamma_\alpha\gamma_\beta v(q_+)\bar{v}(P_+)\gamma^\beta\gamma^\alpha u(P_-) I \\ & + \text{similar terms from second (crossed) Feynman diagram} \ . \end{aligned} \tag{B1}$$

With the aid of the algebraic computation package REDUCE, the six independent helicity amplitudes are found to be

$$
\begin{aligned}
iM_{++++}=&2mm_1\{2E^2Y[PP_1(2\cos\theta-1)+m^2+m_1^2-3E^2]+4E^2G(2E^2-m_1^2)\\
&-2E^2Y'[PP_1(2\cos\theta+1)-m^2-m_1^2+3E^2]+4E^2H(2E^2-m^2)-8E^2PP_1\cos\theta B\\
&+2(E^2+PP_1)(X+X')+E^2(2U_1+2U_2-U_3-U_3')\}/E^2PP_1\ ,\\
iM_{++--}=&-2mm_1\{2E^2Y'[PP_1(2\cos\theta-1)-m^2-m_1^2+3E^2]-4E^2G(2E^2-m_1^2)\\
&-2E^2Y[PP_1(2\cos\theta+1)+m^2+m_1^2-3E^2]\\
&-4E^2H(2E^2-m^2)+8E^2PP_1\cos\theta B-2(E^2-PP_1)(X+X')\\
&-E^2(2U_1+2U_2-U_3-U_3')\}/E^2PP_1\ ,\\
iM_{+++-}=&2m_1E\{-2Y[PP_1\cos\theta(2m^2+m_1^2-4E^2)+P^2P_1^2(3-2\sin^2\theta)+E^2P^2]\\
&-2Y'[PP_1\cos\theta(2m^2+m_1^2-4E^2)-P^2P_1^2(3-2\sin^2\theta)-E^2P^2]\\
&+4PP_1\cos\theta G(m_1^2-2E^2)-8P^3P_1\cos\theta H-8P^2P_1^2\sin^2\theta B-2PP_1\cos\theta U_1\\
&+(2X-U_3)(P^2-PP_1\cos\theta)-(2X'-U_3')(P^2+PP_1\cos\theta)\}/P^2P_1^2\sin\theta\ ,\\
iM_{+-++}=&2mE\{2Y[PP_1\cos\theta(2m_1^2+m^2-4E^2)+P^2P_1^2(3-2\sin^2\theta)+E^2P_1^2]\\
&+2Y'[PP_1\cos\theta(2m_1^2+m^2-4E^2)-P^2P_1^2(3-2\sin^2\theta)-E^2P_1^2]\\
&-4PP_1\cos\theta H(m^2-2E^2)+8PP_1^3\cos\theta G+8P^2P_1^2\sin^2\theta B\\
&+2PP_1\cos\theta U_2-(2X-U_3)(P_1^2-PP_1\cos\theta)+(2X'-U_3')(P_1^2+PP_1\cos\theta)\}/P^2P_1^2\sin\theta\ ,\\
iM_{+-+-}=&2\{2E^2Y[2P^2P_1^2\cos\theta\sin^2\theta(E^2+PP_1)+E^2(E^2+PP_1)(P+P_1)^2(1-\cos\theta)\\
&+PP_1\sin^2\theta(m^2m_1^2+m_1^2E^2+m^2E^2-4E^4-4E^2PP_1)]\\
&+2E^2Y'[-2P^2P_1^2\cos\theta\sin^2\theta(E^2-PP_1)-E^2(E^2-PP_1)(P-P_1)^2(1-\cos\theta)\\
&+PP_1\sin^2\theta(m^2m_1^2+m_1^2E^2+m^2E^2-4E^4+4E^2PP_1)]\\
&+4E^4PP_1G[2P_1^2\sin^2\theta-(E^2+P_1^2)(1-\cos\theta)]+4E^4PP_1H[2P^2\sin^2\theta-(E^2+P^2)(1-\cos\theta)]\\
&-8E^4P^2P_1^2\sin^2\theta(1+\cos\theta)B+E^2(E^2+PP_1)U_3[(P+P_1)^2(1-\cos\theta)-PP_1\sin^2\theta]\\
&-E^2(E^2-PP_1)U_3'[(P-P_1)^2(1-\cos\theta)+PP_1\sin^2\theta]-2E^2PP_1U_2(E^2+P^2)(1-\cos\theta)\\
&-2E^2PP_1U_1(E^2+P_1^2)(1-\cos\theta)-2X(E^2+PP_1)[E^2(P+P_1)^2(1-\cos\theta)-PP_1(E^2+PP_1)\sin^2\theta]\\
&+2X'(E^2-PP_1)[E^2(P-P_1)^2(1-\cos\theta)+PP_1(E^2-PP_1)\sin^2\theta]\}/E^2P^2P_1^2\sin^2\theta\ ,\\
iM_{+--+}=&-2\{-2E^2Y'[2P^2P_1^2\cos\theta\sin^2\theta(E^2+PP_1)-E^2(E^2+PP_1)(P+P_1)^2(1+\cos\theta)\\
&-PP_1\sin^2\theta(m^2m_1^2+m_1^2E^2+m^2E^2-4E^4-4E^2PP_1)]\\
&-2E^2Y[-2P^2P_1^2\cos\theta\sin^2\theta(E^2-PP_1)+E^2(E^2-PP_1)(P-P_1)^2(1+\cos\theta)\\
&-PP_1\sin^2\theta(m^2m_1^2+m_1^2E^2+m^2E^2-4E^4+4E^2PP_1)]\\
&+4E^4PP_1G[2P_1^2\sin^2\theta-(E^2+P_1^2)(1+\cos\theta)]+4E^4PP_1H[2P^2\sin^2\theta-(E^2+P^2)(1+\cos\theta)]\\
&+8E^4P^2P_1^2\sin^2\theta(1-\cos\theta)B+E^2(E^2+PP_1)U_3'[(P+P_1)^2(1+\cos\theta)-PP_1\sin^2\theta]\\
&-E^2(E^2-PP_1)U_3[(P-P_1)^2(1+\cos\theta)+PP_1\sin^2\theta]-2E^2PP_1U_2(E^2+P^2)(1+\cos\theta)\\
&-2E^2PP_1U_1(E^2+P_1^2)(1+\cos\theta)\\
&-2X'(E^2+PP_1)[E^2(P+P_1)^2(1+\cos\theta)-PP_1(E^2+PP_1)\sin^2\theta]\\
&+2X(E^2-PP_1)[E^2(P-P_1)^2(1+\cos\theta)+PP_1(E^2-PP_1)\sin^2\theta]\}/E^2P^2P_1^2\sin^2\theta\ ,
\end{aligned}
\tag{B2}
$$

where

$$U_1=S-N,\ U_2=S-L,\ U_3=S-R,\ U_3'=S-R',$$

$$B=(E^2-PP_1\cos\theta)I-(E^2+PP_1\cos\theta)I',$$

and

$$Y=F-2E^2I.$$

APPENDIX C: PARTIAL-WAVE ANALYSIS AND THE UNITARITY CONDITION

The imaginary parts of the partial-wave amplitudes may be evaluated in one of two ways: (i) by direct integration of the imaginary parts of the helicity amplitudes with the appropriate Wigner d functions; (ii) by utilizing the unitarity condition and the partial-wave amplitudes of the processes $q\bar{q}\to gg$ and $gg\to Q\bar{Q}$. The latter is much simpler and gives far more transparent results.

For $q\bar{q}\to gg\to Q\bar{Q}$, let the direction of the $q\bar{q}$ pair define the z axis (assuming center-of-momentum kinematics). Let the gluons for both $q\bar{q}\to gg$ and $gg\to Q\bar{Q}$ travel along the line defined by the polar angles θ' and ϕ', and let the direction of travel of the $Q\bar{Q}$ pair be defined by the angle θ.

Now, consider a general helicity amplitude, M, for $q\bar{q}\to gg$. Let a, b be the helicities of $q\bar{q}$, and a',b' be those of the gg pair. Then this helicity amplitude may be expanded in partial-wave amplitudes

$$M^{(1)}_{a'b';ab}(\theta',\phi')=\sum_J(2J+1)D^{J*}_{\mu'\mu}(\phi',\theta',-\phi')T^{(1)J}_{\mu'\mu}/(4\pi)\ , \tag{C1}$$

where $D^J_{\mu'\mu}$ are the rotation matrices, $\mu'=a'-b'$, $\mu=a-b$, and

$$T^{(1)J}_{\mu'\mu}=\int M^{(1)}_{a'b';ab}(\theta',\phi')D^J_{\mu'\mu}(\phi',\theta',-\phi')d\Omega'\ . \tag{C2}$$

Similarly, the helicity amplitude for the process $gg\to Q\bar{Q}$ may be written

$$M^{(2)}_{cd;a'b'}(\theta',\phi',\theta)=\sum_{J,m}(2J+1)D^{J*}_{\nu m}(0,\theta,0)\times D^J_{\mu'm}(\phi',\theta',-\phi')\times T^{(2)J}_{\nu\mu'}/(4\pi)\ , \tag{C3}$$

where

$$T^{(2)J}_{\nu\mu'}=\int M^{(2)}_{cd;a'b'}(\theta',\phi',\theta)D^J_{\nu m}(0,\theta,0)\times D^{J*}_{\mu'm}(\phi',\theta',-\phi')d\Omega' d\Omega\ . \tag{C4}$$

$\nu=c-d$, and c,d are the helicities of the final-quark pair.

The imaginary part of the helicity amplitude for $q\bar{q}\to gg\to Q\bar{Q}$ is obtained from the previous two by multiplying, summing over the gluon helicity states (μ'), and integrating over the gluon phase space $d\Omega'$. That is[22]

$$M^{(3)}_{cd;ab}(\theta)=\frac{1}{4\pi}\sum_{\mu',J,J',m}(2J+1)(2J'+1)[T^{(1)J}_{\mu'\mu}T^{(2)J'}_{\nu\mu'}/(16\pi^2)]D^{J*}_{\nu m}(0,\theta,0)\int d\Omega' D^{J*}_{\mu'\mu}(\phi',\theta',-\phi')D^{J'}_{\mu'm}(\phi',\theta',-\phi')$$

$$=\frac{1}{4\pi}\sum_{\mu'}\sum_{J,J',m}(2J+1)(2J'+1)[T^{(1)J}_{\mu'\mu}T^{(2)J'}_{\nu\mu'}D^{J*}_{\nu m}(0,\theta,0)/(16\pi^2)]\frac{1}{2\pi}\frac{8\pi^2}{2J+1}\delta_{JJ'}\delta_{\mu'\mu'}\delta_{\mu m}$$

$$=\frac{1}{4\pi}\sum_{J,\mu'}(2J+1)T^{(1)J}_{\mu'\mu}T^{(2)J}_{\nu\mu'}D^{J*}_{\nu\mu}(0,\theta,0)/(4\pi)\ , \tag{C5}$$

where the $1/(2\pi)$ inside the summation arises because there is no integration over one of the three Euler angles; it has been chosen to be zero. The superscripts (1), (2), and (3) are present only to distinguish among the helicity amplitudes for the three different processes being discussed.

The imaginary parts of the helicity amplitudes for the process $q\bar{q}\to gg\to Q\bar{Q}$, evaluated without use of the unitarity condition, may be expanded

$$M^{(3)}_{cd;ab}(\theta)=\sum_J(2J+1)D^{J*}_{\nu\mu}(0,\theta,0)T^{(3)J}_{\nu\mu}/(4\pi)\ , \tag{C6}$$

and comparison of Eq. (C6) with the previous expansion of Eq. (C5) indicates that the imaginary parts of the partial-wave amplitudes for the process $q\bar{q}\to gg\to Q\bar{Q}$ may be written in terms of the partial-wave amplitudes for $q\bar{q}\to gg$ and $gg\to Q\bar{Q}$ as

$$T^{(3)J}_{\nu\mu}=\frac{1}{4\pi}\sum_{\mu'}T^{(1)J}_{\mu'\mu}T^{(2)J}_{\nu\mu'}\ . \tag{C7}$$

Using the partial-wave amplitudes of Refs. 12 and 13, the imaginary parts of the partial-wave amplitudes for $q\bar{q}\to gg\to Q\bar{Q}$ for $J\le 4$ are

$$T^J_{\mu\nu}=T^J_{\lambda_3\lambda_4\lambda_1\lambda_2}\ ,$$

where J is the total angular momentum,

$$iT^0_{++++}=-g^4mm_1(E^2+PP_1)A_1A_2/4E^4vv_1,\quad iT^0_{++--}=g^4mm_1(E^2-PP_1)A_1A_2/4E^4vv_1\ ,$$

$$\begin{aligned}iT^2_{++++}=-mm_1g^4\{&3A_1A_2[2(E^2+PP_1)v^2v_1^2(3-v^2)(3-v_1^2)+3PP_1(1-v^2)^2(1-v_1^2)^2]\\&+6v_1A_1[PP_1(1-v^2)^2(5v_1^2-3)-6(E^2+PP_1)v^2v_1^2(3-v^2)]\\&+6vA_2[PP_1(1-v_1^2)^2(5v^2-3)-6(E^2+PP_1)v^2v_1^2(3-v_1^2)]\\&+4vv_1[54(E^2+PP_1)v^2v_1^2+PP_1(5v^2-3)(5v_1^2-3)]\}/96E^4v^5v_1^5\ ,\end{aligned}$$

$$\begin{aligned}iT^2_{++--}=mm_1g^4\{&3A_1A_2[2(E^2-PP_1)v^2v_1^2(3-v^2)(3-v_1^2)-3PP_1(1-v^2)^2(1-v_1^2)^2]\\&-6v_1A_1[PP_1(1-v^2)^2(5v_1^2-3)+6(E^2-PP_1)v^2v_1^2(3-v^2)]\\&-6vA_2[PP_1(1-v_1^2)^2(5v^2-3)-6(E^2-PP_1)v^2v_1^2(3-v_1^2)]\\&+4vv_1[54(E^2-PP_1)v^2v_1^2-PP_1(5v^2-3)(5v_1^2-3)]\}/96E^4v^5v_1^5\ ,\end{aligned}$$

$$iT^2_{+++-}=\sqrt{6}g^4m_1PP_1[3A_1(1+v^2)(1-v^2)-2v(3+v^2)][3A_2(1-v_1^2)^2+2v_1(5v_1^2-3)]/288E^3v^5v_1^5\ ,$$

$$iT^2_{+-++}=\sqrt{6}g^4mPP_1[3A_2(1+v_1^2)(1-v_1^2)-2v_1(3+v_1^2)][3A_1(1-v^2)^2+2v(5v^2-3)]/288E^3v^5v_1^5\ ,$$

$$iT^2_{+-+-}=g^4PP_1[2v(v^2+3)-3(1+v^2)(1-v^2)A_1][2v_1(v_1^2+3)-3(1+v_1^2)(1-v_1^2)A_2]/144E^2v^5v_1^5\ ,$$

$$iT^3_{+-+-}=5g^4PP_1[2v(13v^2-15)+3(1-v^2)(5-v^2)A_1][2v_1(13v_1^2-15)+3(1-v_1^2)(5-v_1^2)A_2]/1152E^2v^5v_1^5\ ,$$

$$\begin{aligned}iT^4_{++++}=-g^4mm_1\{&45A_1A_2[(E^2+PP_1)(3v^4-30v^2+35)(3v_1^4-30v_1^2+35)+10PP_1(1-v^2)^2(7-v^2)(1-v_1^2)^2(7-v_1^2)]\\&+30A_1v_1[5(E^2+PP_1)(11v_1^2-21)(3v^4-30v^2+35)v^2v_1^2\\&-2PP_1(1-v^2)^2(7-v^2)(81v_1^4-190v_1^2+105)]\\&+30A_2v[5(E^2+PP_1)(11v^2-21)(3v_1^4-30v_1^2+35)\\&\qquad-2PP_1(1-v_1^2)(7-v_1^2)(81v^4-190v^2+105)]\\&+4vv_1[125(E^2+PP_1)v^2v_1^2(11v^2-21)(11v_1^2-21)+2PP_1(81v^4-190v^2+105)\\&\qquad\times(81v_1^4-190v_1^2+105)]\}/11\,520E^4v^7v_1^7\ ,\end{aligned}$$

$$\begin{aligned}iT^4_{++--}=-g^4mm_1\{&45A_1A_2[(E^2-PP_1)(3v^4-30v^2+35)(3v_1^4-30v_1^2+35)\\&\qquad-10PP_1(1-v^2)^2(7-v^2)(1-v_1^2)^2(7-v_1^2)]\\&+30A_1v_1[5(E^2-PP_1)(11v_1^2-21)(3v^4-30v^2+35)v^2v_1^2\\&\qquad+2PP_1(1-v^2)^2(7-v^2)(81v_1^4-190v_1^2+105)]\\&+30A_2v[5(E^2-PP_1)(11v^2-21)(3v_1^4-30v_1^2+35)+2PP_1(1-v_1^2)(7-v_1^2)(81v^4-190v^2+105)]\\&+4vv_1[125(E^2-PP_1)v^2v_1^2(11v^2-21)(11v_1^2-21)\\&\qquad-2PP_1(81v^4-190v^2+105)(81v_1^4-190v_1^2+105)]\}/11\,520E^4v^7v_1^7\ ,\end{aligned}$$

$$\begin{aligned}iT^4_{+++-}=\sqrt{5}\,g^4m_1PP_1&[15(1-v^2)(v^4+v^2-14)A_1-2v(33v^4+155v^2-210)]\\&\times[15(1-v_1^2)^2(7-v_1^2)A_2-2v_1(81v_1^4-190v_1^2+105)]/28\,800E^3v^7v_1^7\ ,\end{aligned}$$

$$\begin{aligned}iT^4_{+-++}=-\sqrt{5}g^4mPP_1&[15(1-v_1^2)(v_1^4+v_1^2-14)A_2-2v_1(33v_1^4+155v_1^2-210)]\\&\times[15(1-v^2)^2(7-v^2)A_1-2v(81v^4-190v^2+105)]/28\,800E^3v^7v_1^7\ ,\end{aligned}$$

$$\begin{aligned}iT^4_{+-+-}=g^4PP_1&[15(1-v^2)(v^4+v^2-14)A_1-2v(33v^4+155v^2-210)]\\&\times[15(1-v_1^2)(v_1^4+v_1^2-14)A_2-2v_1(33v_1^4+155v_1^2-210)]/28\,800E^2v^7v_1^7\ ,\end{aligned}$$

where

$$A_1=\ln\frac{1+v}{1-v},\quad A_2=\ln\frac{1+v_1}{1-v_1}\ .$$

*Present address: Institut des Sciences Nucléaires, 53, Avenue des Martyrs, 38026 Grenoble Cedex, France.

[1]S. Okubo, Phys. Lett. **5**, 165 (1963); G. Zweig, CERN Reports Nos. TH401, 1964 and TH402, 1965 (unpublished); in *Symmetries in Elementary Particle Physics,* proceedings of the International School of Physics, "Ettore Majorana," Erice, Italy, 1964, edited by A. Zichichi (Academic, New York, 1965); J. Iizuka, Prog. Theor. Phys. Suppl. **37-38**, 21 (1966).
[2]See, for example, H. Genz and S. Tatur, Phys. Rev. D **30**, 63 (1984).
[3]L. Micu, Nucl. Phys. **B10**, 521 (1969).
[4]A. M. Green, J. S. Niskanen, and S. Wycech, Phys. Lett. B **172**, 171 (1987); J. S. Niskanen, talk given at the proceedings of the 1988 Lake Louise Winter Institute, Lake Louise, Canada (in press).
[5]M. Jacob and G. C. Wick, Ann. Phys. (N.Y.) **7**, 404 (1959).
[6]A. D. Martin and T. D. Spearman, *Elementary Particle Theory* (Benjamin/Cummings, Reading, MA, 1981).
[7]F. A. Berends, K. J. F. Gaemers, and R. Gastmans, Nucl. Phys. **B57**, 381 (1973); **B63**, 381 (1973).
[8]W. Roberts, University of Guelph, Ph.D. thesis, 1988.
[9]W. Marciano and H. Pagels, Phys. Rep. **36C**, 137 (1978).
[10]L. Lewin, *Polylogarithms and Associated Functions* (North-Holland, New York, 1981).
[11]L. D. Landau and E. M. Lifshitz, *Course of Theoretical Physics* (Pergamon, London, 1981), Vol. 3.
[12]W. Roberts, Can. J. Phys. **64**, 1359 (1986).
[13]W. Roberts, Can. J. Phys. **64**, 1514 (1986).
[14]See, for example, V. A. Novikov *et al.*, Phys. Rep. **41C**, 1 (1978).
[15]See, for example, E. D. Bloom, J. Phys. (Paris) Colloq. **43**, C3-407 (1982).
[16]G. Karl, W. Roberts, and N. Zagury, Phys. Lett. **149B**, 403 (1984).
[17]W. Roberts and G. Karl (unpublished).
[18]G. 't Hooft and M. Veltman, Nucl. Phys. **B44**, 189 (1972).
[19]G. Leibbrandt, Rev. Mod. Phys. **4**, 849 (1975).
[20]S. Narison, Phys. Rep. **82**, 263 (1982).
[21]F. J. Yndurain, *Quantum Chromodynamics* (Springer, New York, 1983).
[22]D. A. Varshalovich, A. H. Moskalev, and V. K. Hersonskii, *Kvantovaya Teoriia Uglovoga Momenta* (Nauka, Leningrad, 1975).